nature immunology

Essential function for the calcium sensor STIM1 in mast cell activation and anaphylactic responses

Yoshihiro Baba[1], Keigo Nishida[2], Yoko Fujii[1], Toshio Hirano[2], Masaki Hikida[1] & Tomohiro Kurosaki[1]

Mast cells have key functions as effectors of immunoglobulin E–mediated allergic inflammatory diseases. Allergen stimulation induces Ca^{2+} influx and elicits the secretion of inflammatory mediators from mast cells. Here we show that the Ca^{2+}-binding endoplasmic reticulum protein STIM1 is critical to mast cell function. STIM1-deficient fetal liver–derived mast cells had impaired Ca^{2+} influx mediated by the high-affinity immunoglobulin E receptor FcεRI and activation of the transcription factors NF-κB and NFAT. Mast cells lacking STIM1 also had much less degranulation and cytokine production after FcεRI stimulation. In addition, alterations in STIM1 expression affected the sensitivity of immunoglobulin E–mediated immediate-phase anaphylactic responses *in vivo*. Thus, STIM1 is key in promoting the Ca^{2+} influx that is essential for FcεRI-mediated mast cell activation and anaphylaxis.

Mast cells are the main effector cells in immediate hypersensitivity reactions and allergic diseases that are associated with immunoglobulin E (IgE) and dependent on T helper type 2 (T_H2) cells, as well as in certain innate immune responses[1,2]. Mast cells express the high-affinity IgE receptor FcεRI, and binding of multivalent antigen to FcεRI-bound IgE induces receptor aggregation and triggers mast cell activation[3]. Activated mast cells secrete preformed mediators, including proteases and vasoactive amines such as histamine, that are stored in cytoplasmic granules. In addition, mast cell activation results in the *de novo* synthesis of proinflammatory lipid mediators and cytokines. The signaling pathways that mediate the synthesis and release of such mediators in response to FcεRI aggregation involve multiple protein tyrosine kinase cascades.

One important 'downstream' target of such cascades is phospholipase C-γ (PLC-γ), which catalyzes the hydrolysis of phosphatidylinositol-4,5-bisphosphate to diacylglycerol and inositol-1,4,5-trisphosphate ($Ins(1,4,5)P_3$). $Ins(1,4,5)P_3$ binds to its receptor in the endoplasmic reticulum membrane, thereby causing a rapid but transient release of Ca^{2+} from endoplasmic reticulum stores. The second stage of calcium mobilization involves a sustained influx of extracellular Ca^{2+} across the plasma membrane. Initiation of this second step has been thought to result directly from the emptying of endoplasmic reticulum Ca^{2+} stores, which activates Ca^{2+} channels in the plasma membrane; collectively these processes are called 'store-operated Ca^{2+} (SOC) influx'[4,5]. However, other mechanisms of activating Ca^{2+} channels in the plasma membrane independently of the depletion of endoplasmic reticulum Ca^{2+} stores have been reported[4–6].

In mast cells, SOC influx is mediated by calcium release–activated calcium (CRAC) channels[4,5,7,8], which have the unique characteristics of high Ca^{2+} sensitivity combined with low conductance. The identification of Orai1 (also called CRACM1), a component of the CRAC channel[9–11], and STIM1, a sensor of endoplasmic reticulum Ca^{2+} concentrations that couples depletion of endoplasmic reticulum Ca^{2+} stores with SOC influx[12,13], has provided long-awaited insight into the molecular basis of CRAC currents. STIM1, a type I endoplasmic reticulum membrane protein, has an amino-terminal 'EF-hand' Ca^{2+}-binding domain that resides in the lumen of the endoplasmic reticulum. The depletion of endoplasmic reticulum Ca^{2+} stores results in the relocation of STIM1 into puncta under the plasma membrane and subsequent activation of SOC channels[13–18]. The initiation of SOC influx requires the sterile α-motif, coiled-coil and serine-threonine–rich domains of STIM1 (ref. 14) and may involve the formation of STIM1 multimers[19].

The importance of Ca^{2+} influx in mast cell activation and degranulation is widely accepted, mainly on the basis of pharmacological experiments; treatment with the Ca^{2+} chelator EGTA almost completely abolishes FcεRI-mediated Ca^{2+} mobilization and degranulation[20,21]. However, additional evidence indicates that despite their defective Ca^{2+} mobilization, mast cells lacking the Src tyrosine kinase Lyn nonetheless undergo IgE-mediated degranulation[22–25]. Thus, it remains unclear whether the second stage of Ca^{2+} mobilization (Ca^{2+} influx) is indeed essential for mast cell activation and degranulation. Even if so, it remains unknown whether the SOC pathway is important in mast cell responses, as both SOC-dependent and SOC-independent pathways are thought to coexist[4–6,26].

To directly assess the involvement of SOC influx in mast cell activation, we generated STIM1-deficient mice. We found that STIM1 critically regulated FcεRI-induced Ca^{2+} influx as well as activation of the transcription factors NF-κB and NFAT, degranulation

[1]Laboratory for Lymphocyte Differentiation and [2]Laboratory for Cytokine Signaling, RIKEN Research Center for Allergy and Immunology, 1-7-22, Suehirocho, Tsurumi-ku, Yokohama, Kanagawa 230-0045, Japan. Correspondence should be addressed to T.K. (kurosaki@rcai.riken.jp).

Received 23 August; accepted 6 November; published online 2 December 2007; doi:10.1038/ni1546

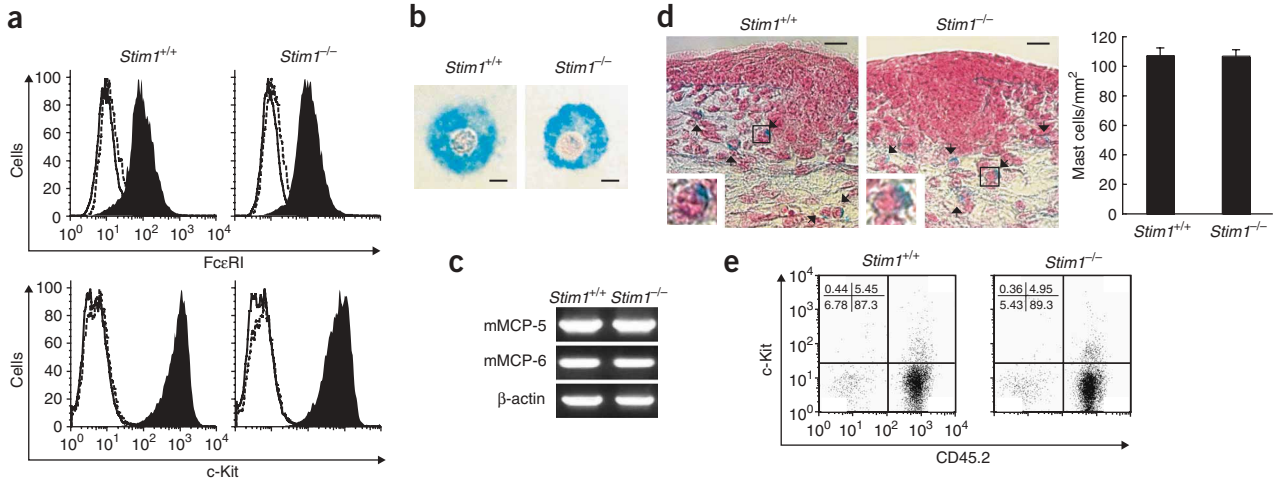

Figure 1 Development of *Stim1*$^{-/-}$ mast cells. (**a**) Flow cytometry of the surface expression of FcεRI and c-Kit (filled histograms) on FLMCs from *Stim1*$^{+/+}$ and *Stim1*$^{-/-}$ mice. Solid lines, unstained; dotted lines, isotype control. (**b**) Staining of cytospin preparations with nuclear fast red and alcian blue. Scale bars, 2 μm. (**c**) RT-PCR of mRNA encoding mMCP-5, mMCP-6 and β-actin in *Stim1*$^{+/+}$ and *Stim1*$^{-/-}$ FLMCs. (**d**) Histological analysis of tissue mast cells in skin from *Stim1*$^{+/+}$ and *Stim1*$^{-/-}$ E15.5 embryos. Sections were stained with nuclear fast red and alcian blue. Arrowheads indicate mast cells stained with alcian blue. Insets (bottom left corners) show mast cells in boxes in main images. Original magnification, ×60 (main images) or ×100 (insets); scale bars, 10 μm. Graph (right), absolute numbers of mast cells per mm^2 (mean + s.d.). (**e**) Mast cell differentiation *in vivo* of cells from *Stim1*$^{+/+}$ and *Stim1*$^{-/-}$ E15.5 fetal livers (CD45.2$^+$; 2 × 10^6 cells) injected into lethally irradiated congenic mice (CD45.1$^+$), then isolated from the peritoneal cavity after 10 weeks and analyzed by flow cytometry. Numbers in plots indicate percent cells in each quadrant. Data are representative of at least two independent experiments.

and *in vivo* anaphylaxis responses. Our data provide direct genetic evidence of the importance of STIM1 in mast cell activation.

RESULTS

Mast cell development in *Stim1*$^{-/-}$ mice

To investigate the physiological function of STIM1 in mast cells and allergic responses, we disrupted *Stim1* in C57BL/6 mice with a Cre recombinase–*lox*P gene-targeting strategy (**Supplementary Fig. 1a** online). We confirmed homologous recombination and Cre-mediated excision of exon 6, which encodes the transmembrane region of STIM1, by Southern blot analysis (**Supplementary Fig. 1b**). We confirmed ablation of STIM1 protein expression in fetal liver cells and fetal liver–derived mast cells (FLMCs) from *Stim1*$^{-/-}$ mice by immunoblot analysis (**Supplementary Fig. 1c,d**). In addition, STIM1 protein was much lower in *Stim1*$^{+/-}$ cells. *Stim1*$^{-/-}$ mice died perinatally of unknown causes, but *Stim1*$^{-/-}$ embryos at embryonic day 18.5 (E18.5) had no obvious abnormalities. In a few cases, *Stim1*$^{-/-}$ mice were born; they were slightly smaller than their *Stim1*$^{+/+}$ littermates but died of apparent respiratory failure within 1 d.

Because of the embryonic death of *Stim1*$^{-/-}$ mice, we collected cell suspensions from the livers of E15.5 embryos and cultured the cells in interleukin 3 (IL-3) to generate highly pure mast cell populations, as assessed by surface expression of FcεRI and c-Kit (**Fig. 1a**). Alcian blue staining of cytospin slides showed that the morphology of *Stim1*$^{-/-}$ mast cells was not different from that of *Stim1*$^{+/+}$ mast cells (**Fig. 1b**). Moreover, mast cell–specific genes, including those encoding the serine proteases mMCP-5 and mMCP-6, were expressed in similar amounts in *Stim1*$^{-/-}$ and *Stim1*$^{+/+}$ FLMCs (**Fig. 1c**).

To compare the differentiation of *Stim1*$^{+/+}$ and *Stim1*$^{-/-}$ mast cells *in vivo*, we counted tissue mast cells in *Stim1*$^{+/+}$ and *Stim1*$^{-/-}$ embryos. The densities of skin mast cells on the backs of *Stim1*$^{+/+}$ and *Stim1*$^{-/-}$ E15.5 embryos were similar (**Fig. 1d**). In addition, we transplanted fetal liver cells of *Stim1*$^{+/+}$ and *Stim1*$^{-/-}$ embryos (CD45.2$^+$) into lethally irradiated congenic mice (CD45.1$^+$) and analyzed hematopoietic reconstitution by flow cytometry. Chimerism in the peripheral blood of mice reconstituted with *Stim1*$^{+/+}$ and *Stim1*$^{-/-}$ cells was almost equal (over 90%; data not shown), indicating that the engraftment of hematopoietic stem cells from *Stim1*$^{-/-}$ embryos was normal. Flow cytometry of peritoneal cavity cells showed intact development of *Stim1*$^{-/-}$ mast cells (**Fig. 1e**). These results collectively suggest that mast cell differentiation is not impaired in the absence of STIM1.

Impaired SOC influx in *Stim1*$^{-/-}$ FLMCs

Studies of HeLa and Jurkat cells based on RNA-mediated interference[12,13] and gene-targeting experiments with DT40 B cells[14] indicate that STIM1 is required for SOC influx. To determine the effect of STIM1 on SOC influx in primary mast cells, we monitored cytosolic Ca^{2+} in *Stim1*$^{+/+}$ and *Stim1*$^{-/-}$ FLMCs. After treating the cells with thapsigargin, a endoplasmic reticulum Ca^{2+} pump inhibitor, in the presence of 0.5 mM EGTA (to deplete Ca^{2+} stores), we added 2 mM Ca^{2+} and monitored Ca^{2+} influx. We noted considerable suppression of Ca^{2+} influx in *Stim1*$^{-/-}$ FLMCs (**Fig. 2a**). We also noted impaired Ca^{2+} influx in *Stim1*$^{-/-}$ FLMCs stimulated with IgE and cognate antigen, instead of thapsigargin, which suggested that STIM1-dependent SOC influx is the main mechanism used during FcεRI signaling (**Fig. 2a**). To further assess the effect of STIM1 on Ca^{2+} mobilization, we stimulated FcεRI with IgE and antigen in the presence of extracellular Ca^{2+}. *Stim1*$^{+/+}$ FLMCs showed a sharp Ca^{2+} spike followed by a sustained Ca^{2+} plateau (**Fig. 2b**). In contrast, cytosolic Ca^{2+} concentrations were much lower in *Stim1*$^{-/-}$ FLMCs. Similarly, whereas ionomycin-treated *Stim1*$^{+/+}$ FLMCs had a continuously high concentration of Ca^{2+}, Ca^{2+} flux was considerably impaired in *Stim1*$^{-/-}$ FLMCs (**Fig. 2b**). These results showed that in FLMCs, ionomycin-triggered Ca^{2+} influx was dependent on STIM1. Given the published evidence that ionomycin is capable of activating SOC channels in the plasma membrane by depleting endoplasmic reticulum Ca^{2+} stores[27], STIM1 probably functions as a sensor of this ionomycin-dependent Ca^{2+} depletion and relays signals to activate Ca^{2+} influx.

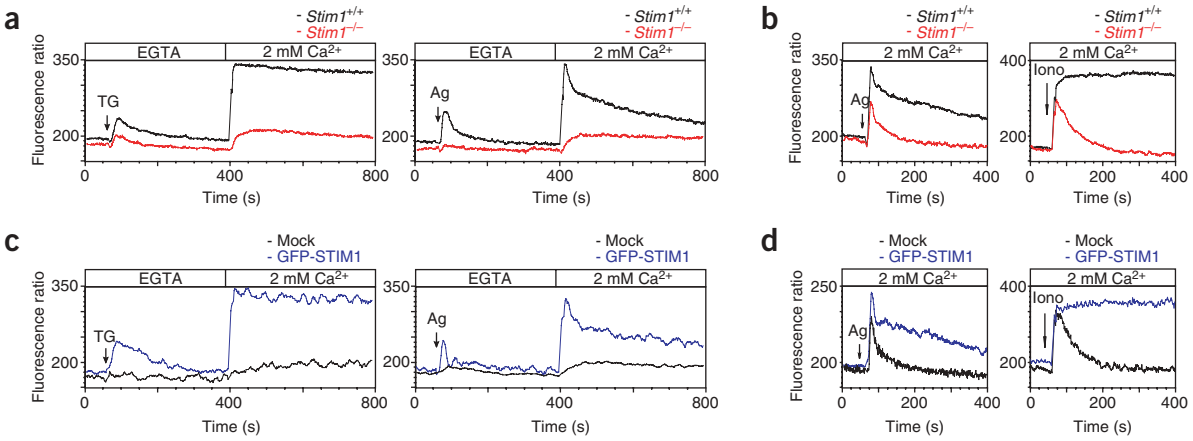

Figure 2 Suppression of SOC influx in *Stim1*$^{-/-}$ FLMCs. (**a**) Ca^{2+}-mobilization profiles, monitored by Indo-1 AM imaging. Ca^{2+} release was elicited in IgE anti-DNP–sensitized FLMCs by stimulation with DNP-HSA (Ag) in Ca^{2+}-free conditions (0.5 mM EGTA), and Ca^{2+} influx was induced by restoration of the extracellular Ca^{2+} concentration to 2 mM in *Stim1*$^{+/+}$ and *Stim1*$^{-/-}$ FLMCs; unsensitized cells were stimulated with thapsigargin (TG) in Ca^{2+}-free conditions before the addition of extracellular Ca^{2+}. (**b**) Ca^{2+}-mobilization profiles in the presence of 2 mM Ca^{2+} in IgE anti-DNP–sensitized *Stim1*$^{+/+}$ and *Stim1*$^{-/-}$ FLMCs after stimulation with DNP-HSA, and in unsensitized FLMCs after treatment with ionomycin (Iono). (**c**,**d**) Ca^{2+}-mobilization profiles of *Stim1*$^{-/-}$ FLMCs retrovirally transduced with GFP alone (Mock) or GFP-STIM1, assessed as described in **a**,**b**. GFP^{+} cells were gated and analyzed. All values are plotted as the FL5/FL4 fluorescence ratio (FL4 = 500–520 nm; FL5 = 400–420 nm). Data are representative of at least three independent experiments.

To confirm that the observed defects in Ca^{2+} influx were due to the absence of STIM1, we retrovirally expressed a green fluorescent protein (GFP)–tagged STIM1 construct (GFP-STIM1) in *Stim1*$^{-/-}$ FLMCs. *Stim1*$^{-/-}$ FLMCs transduced with GFP-STIM1 but not those transduced with GFP alone had restored Ca^{2+} influx induced by FcεRI or thapsigargin stimulation (**Fig. 2c**). Consistent with those results, Ca^{2+} mobilization mediated by IgE aggregation or ionomycin in the presence of 2 mM Ca^{2+} was also restored in *Stim1*$^{-/-}$ FLMCs transduced with GFP-STIM1 (**Fig. 2d**). These results collectively indicate that STIM1 is important in the Ca^{2+} influx induced by the stimulation of mast cells with FcεRI and ionomycin.

STIM1 in mast cell effector functions

FcεRI-mediated mast cell activation induces rapid degranulation and *de novo* synthesis of metabolites and cytokines that are important in allergic reactions. To determine whether such mast cell functions require STIM1, we measured the release of β-hexosaminidase, a protein stored in preformed mast cell granules, from *Stim1*$^{+/+}$ and *Stim1*$^{-/-}$ FLMCs after FcεRI stimulation. STIM1 deficiency resulted in substantial inhibition of antigen-elicited degranulation (**Fig. 3a**). *Stim1*$^{-/-}$ FLMCs also had much less degranulation induced by ionomycin, which is known to bypass FcεRI-proximal signaling and stimulate cells directly by mobilizing free Ca^{2+} ions. The observed differences in β-hexosaminidase release were not due to differences in total β-hexosaminidase content, which was similar in *Stim1*$^{+/+}$ and *Stim1*$^{-/-}$ FLMCs (data not shown). In addition, we confirmed that expression of GFP-STIM1 partially restored the degranulation in *Stim1*$^{-/-}$ FLMCs, as assessed by surface expression of the degranulation marker CD63 (**Supplementary Fig. 2** online). Thus, we concluded that STIM1 was critically required for mast cell degranulation and that a transient Ca^{2+} increase in mast cells was not sufficient to effectively mediate degranulation.

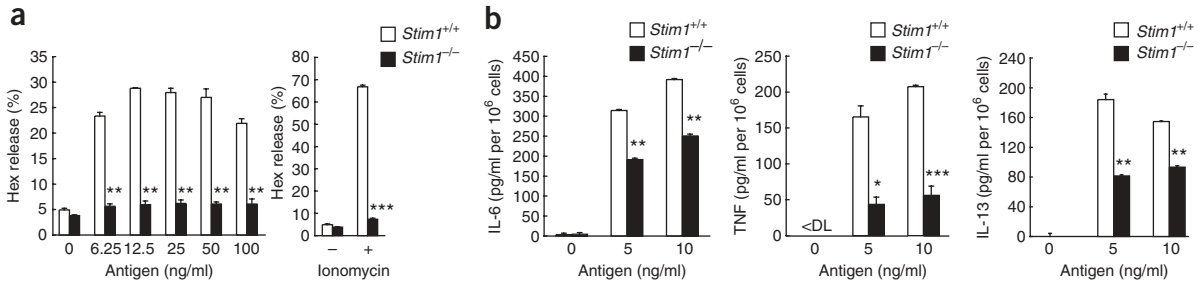

Figure 3 STIM1 is required for FcεRI-induced degranulation and cytokine production. (**a**) Degranulation of *Stim1*$^{+/+}$ and *Stim1*$^{-/-}$ FLMCs, assessed as the release of β-hexosaminidase (Hex) from IgE anti-DNP–sensitized cells after stimulation for 30 min with DNP-HSA (dose, horizontal axis); unsensitized cells (right) were stimulated with 1 μM ionomycin. Data are the mean + s.d. of triplicate samples and are representative of three independent experiments. (**b**) Enzyme-linked immunosorbent assay of the production of IL-6, TNF and IL-13 after stimulation for 3 h with IgE anti-DNP and DNP-HSA (dose, horizontal axis). <DL, below detection limit. Data (mean + s.d.) are representative of three independent experiments. *, $P < 0.05$, **, $P < 0.01$, ***, $P < 0.001$, versus *Stim1*$^{+/+}$ values (**a**,**b**). (**c**) Semiquantitative RT-PCR of mRNA encoding IL-6, TNF, IL-13 and glyceraldehyde phosphate dehydrogenase (GAPDH; loading control) in IgE anti-DNP–sensitized FLMCs stimulated for 1 h with DNP-HSA (5 ng/ml). Data are representative of three independent experiments.

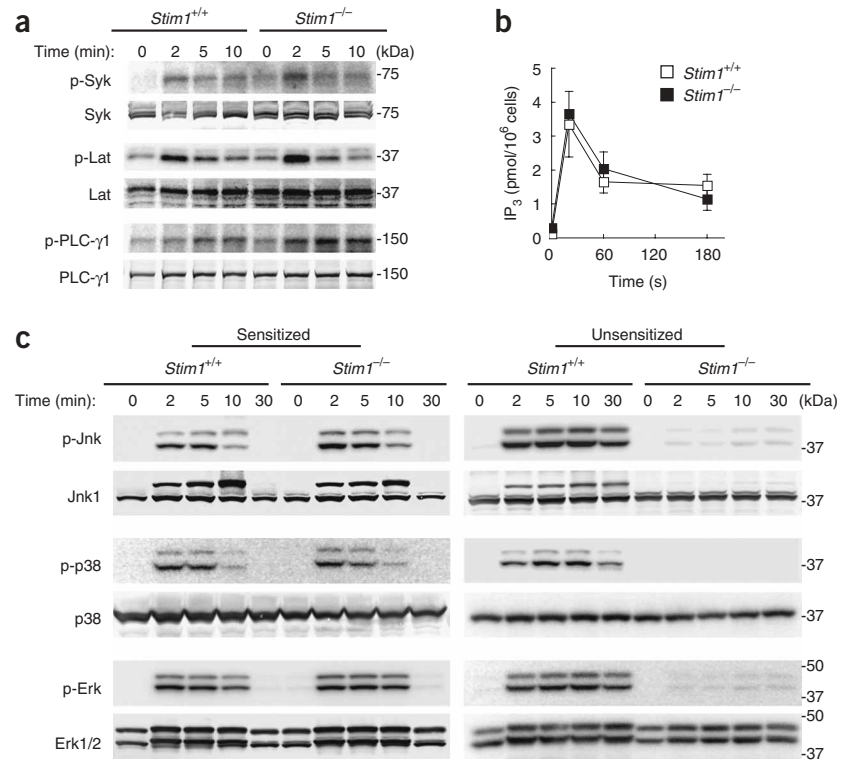

Figure 4 FcεRI-proximal signaling and activation of MAP kinases in *Stim1*$^{+/+}$ and *Stim1*$^{-/-}$ FLMCs. (**a**) Immunoblot analysis of whole-cell lysates of *Stim1*$^{+/+}$ and *Stim1*$^{-/-}$ FLMCs sensitized with IgE anti-DNP and stimulated with DNP-HSA (50 ng/ml; time intervals (left). p-, phosphorylated; right margin, molecular mass standards (in kilodaltons (kDa)). Data are representative of three independent experiments. (**b**) Ins(1,4,5)P_3 (IP_3) production by sensitized *Stim1*$^{+/+}$ and *Stim1*$^{-/-}$ FLMCs stimulated with DNP-HSA. Differences between *Stim1*$^{+/+}$ and *Stim1*$^{-/-}$ FLMCs were not statistically significant. Data are the mean ± s.d. of two independent experiments. (**c**) Immunoblot analysis of sensitized *Stim1*$^{+/+}$ and *Stim1*$^{-/-}$ FLMCs stimulated with DNP-HSA (50 ng/ml; left) and of unsensitized *Stim1*$^{+/+}$ and *Stim1*$^{-/-}$ FLMCs stimulated with 1 μM ionomycin (right). Data are representative of three independent experiments.

To assess the function of STIM1 in mast cell cytokine production, we measured the secretion of IL-6, tumor necrosis factor (TNF) and IL-13 by *Stim1*$^{+/+}$ and *Stim1*$^{-/-}$ FLMCs stimulated with IgE anti-DNP and DNP-HSA. *Stim1*$^{-/-}$ FLMCS produced much less of all three cytokines, as measured by enzyme-linked immunosorbent assay (**Fig. 3b**). Semiquantitative RT-PCR analysis showed that synthesis of mRNA encoding these cytokines was also considerably impaired in the absence of STIM1 (**Fig. 3c**). Therefore, STIM1 is essential for the production and release of IL-6, TNF and IL-13.

FcεRI signaling events in *Stim1*$^{-/-}$ FLMCs

The data presented above suggested that the impaired Ca^{2+} flux in *Stim1*$^{-/-}$ FLMCs might lead to defective intracellular signaling events required for mast cell function. Thus, we examined the activation of various intracellular FcεRI signaling pathways in *Stim1*$^{+/+}$ and *Stim1*$^{-/-}$ FLMCs. We sensitized FLMCs with IgE and stimulated them with antigen for various time periods, then assessed by immunoblot the activation status of FcεRI-proximal molecules, including the tyrosine kinase Syk,

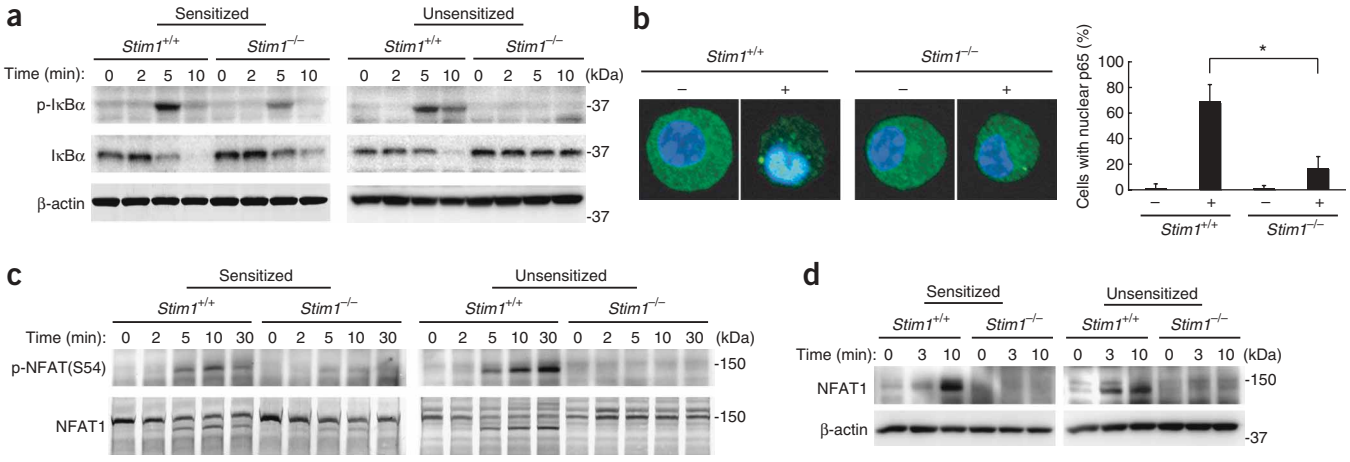

Figure 5 Activation of NF-κB and NFAT is inhibited in *Stim1*$^{-/-}$ FLMCs. (**a**) Immunoblot analysis of IκBα phosphorylation and degradation in whole-cell lysates of *Stim1*$^{+/+}$ and *Stim1*$^{-/-}$ FLMCs sensitized with IgE anti-DNP and stimulated with DNP-HSA (50 ng/ml; left) and in unsensitized *Stim1*$^{+/+}$ and *Stim1*$^{-/-}$ FLMCs stimulated with 1 μM ionomycin (right). (**b**) Confocal microscopy of NF-κB p65 nuclear translocation in *Stim1*$^{+/+}$ and *Stim1*$^{-/-}$ FLMCs sensitized with IgE anti-DNP and stimulated for 10 min with DNP-HSA (100 ng/ml), then fixed and processed for immunofluorescence with anti-p65 (green) and DAPI (4,6-diamidino-2-phenylindole; blue). Scale bar, 5 μm. Right, proportion of cells with p65 nuclear translocation (mean + s.d. of a total of 100 cells counted randomly in each sample). *, $P < 0.001$, versus *Stim1*$^{+/+}$ values. (**c**) Immunoblot analysis of NFAT phosphorylated at Ser54 and NFAT1 in whole-cell lysates of FLMCs stimulated with DNP-HSA (50 ng/ml; left) or 1 μM ionomycin (right) as described in **a**. (**d**) Immunoblot analysis of NFAT1 nuclear translocation in nuclear extracts of cells stimulated with DNP-HSA (50 ng/ml; left) or 1 μM ionomycin (right) as described in **a**. β-actin, loading control. Data are representative of at least three independent experiments.

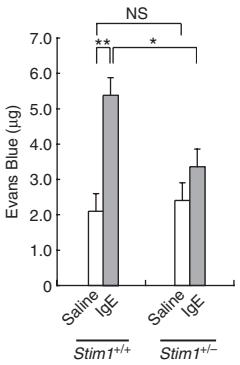

Figure 6 *In vivo* anaphylaxis is lower in *Stim1*$^{+/-}$ mice. Analysis of PCA in *Stim1*$^{+/+}$ mice ($n = 10$) and *Stim1*$^{+/-}$ mice ($n = 8$) injected intradermally in the right ears with IgE anti-DNP and in the left ears with saline (control); after 16–18 h, DNP-HSA was administered intravenously together with Evans blue dye, followed by measurement (mean + s.d.) of the extravasation of Evans blue into the ears. *, $P < 0.05$, and **, $P < 0.01$, versus the corresponding control. NS, not significant. Data are representative of two experiments.

the adaptor molecule Lat, and PLC-γ1. *Stim1*$^{+/+}$ and *Stim1*$^{-/-}$ FLMCs had similar tyrosine phosphorylation of Syk, Lat and PLC-γ1 (**Fig. 4a**). In addition, the absence of STIM1 did not affect the production of Ins(1,4,5)P_3, which is mediated by PLC-γ (**Fig. 4b**). These data indicate that FcεRI-proximal signaling is not globally affected by STIM1.

Mitogen-activated protein (MAP) kinase cascades regulate cytokine production in many cell types[28], but we found that FcεRI-mediated phosphorylation of the MAP kinases Jnk, p38 and Erk was not altered by the absence of STIM1 (**Fig. 4c**). However, whereas a forced increase in cytosolic Ca^{2+} by ionomycin phosphorylated Jnk, p38 and Erk in *Stim1*$^{+/+}$ FLMCs, phosphorylation of these MAP kinases was lower in *Stim1*$^{-/-}$ FLMCs (**Fig. 4c**). Thus, STIM1 is not required for the FcεRI-elicited activation of Jnk, p38 and Erk, but ionomycin-triggerd activation of these MAP kinases is dependent on STIM1.

FcεRI stimulation activates the transcription factors NF-κB and NFAT, which regulate mast cell functions such as cytokine production[29–32]. Because published studies have shown that NF-κB is selectively activated by a large transient increase in Ca^{2+}, whereas NFAT is activated by a low, sustained Ca^{2+} plateau[33,34], we evaluated the contribution of STIM1 to the activation of NF-κB and NFAT. The phosphorylation and degradation of the NF-κB inhibitor IκBα after FcεRI and ionomycin stimulation was much less in *Stim1*$^{-/-}$ FLMCs than in *Stim1*$^{+/+}$ FLMCs (**Fig. 5a**). In addition, FcεRI-mediated nuclear translocation of the NF-κB subunit p65 was much lower in *Stim1*$^{-/-}$ FLMCs (**Fig. 5b**). To examine NFAT activation, we measured the phosphorylation of NFAT residue Ser54, because unlike other residues, whose phosphorylation inhibits NFAT activity, Ser54 phosphorylation enhances NFAT activity[34]. *Stim1*$^{-/-}$ FLMCs had substantially impaired phosphorylation of NFAT after FcεRI and ionomycin stimulation (**Fig. 5c**). Furthermore, we noted much less dephosphorylation of inhibitory serine residues and nuclear translocation of NFAT1 in *Stim1*$^{-/-}$ FLMCs (**Fig. 5c,d**). We conclude that STIM1-dependent Ca^{2+} influx positively regulates the activation of both NF-κB and NFAT in mast cells. Given that NF-κB promotes the expression of IL-6 and TNF[29,30] and NFAT enhances the production of IL-13 and TNF[31,32] in mast cells, impaired NF-κB and NFAT activation may contribute to the insufficient production of these cytokines in *Stim1*$^{-/-}$ FLMCs.

STIM1 in anaphylactic responses *in vivo*

To evaluate whether STIM1 has a function in mast cells *in vivo*, we elicited FcεRI-mediated passive cutaneous anaphylaxis (PCA) reactions in *Stim1*$^{+/+}$ and *Stim1*$^{+/-}$ mice. Because *Stim1*$^{-/-}$ mice die *in utero* and FLMCs from *Stim1*$^{+/-}$ mice expressed much less STIM1 protein than those from *Stim1*$^{+/+}$ mice, we used adult *Stim1*$^{+/-}$ mice as a model of STIM1 insufficiency. We elicited PCA by intradermal injection of IgE antibody to dinitrophenyl (anti-DNP) into the pinna of the right ear. As an internal control, we injected the left ear with an identical volume of saline. After 16–18 h, we challenged the mice by intravenous injection of the antigen DNP–human serum albumin (DNP-HSA) and Evans blue dye. The extravasation of Evans blue dye during the first hour after PCA induction is dependent mainly on the degranulation of activated mast cells, with rapid release of histamine and serotonin resulting in locally increased blood vessel permeability. Extravasation can be quantified by measurement of the amount of dye in tissue biopsies from IgE-treated ears relative to that in ears treated with saline. In control saline-injected ears, Evans blue quantities were not different in *Stim1*$^{+/+}$ and *Stim1*$^{+/-}$ mice (**Fig. 6**). However, extravasation in the IgE-treated pinnae of *Stim1*$^{+/-}$ mice was significantly lower than that in *Stim1*$^{+/+}$ mice (**Fig. 6**), which suggested that STIM1 is required for antigen-induced mast cell–mediated PCA reactions *in vivo*.

DISCUSSION

Here we have shown, by genetic ablation, that STIM1 is an essential positive regulator of mast cell activation and effector function. Although mast cells seemed to differentiate normally in the absence of STIM1, this molecule was critically required for Ca^{2+} influx and subsequent activation of NF-κB and NFAT induced by ligation of the high-affinity IgE receptor FcεRI. Accordingly, loss of STIM1 impaired mast cell degranulation, production of NF-κB- and NFAT-regulated proinflammatory cytokines (IL-6, TNF and IL-13), and immediate-type allergic reactions *in vivo*.

Studies have shown that STIM1 functions as a sensor of Ca^{2+} in the endoplasmic reticulum and ultimately activates plasma membrane SOC channels after depletion of endoplasmic reticulum Ca^{2+} stores. In some tissues, SOC-independent Ca^{2+} influx pathways are thought to exist, thereby raising the issue of whether SOC influx is a key mechanism active in mast cells. In our study, the sustained increase in intracellular free Ca^{2+} concentrations after FcεRI stimulation was almost completely abrogated in *Stim1*$^{-/-}$ mast cells. Moreover, in agreement with previous evidence that ionomycin is able to activate SOC channels by depleting endoplasmic reticulum Ca^{2+} stores, ionomycin was incapable of sustaining Ca^{2+} influx in the absence of STIM1 in mast cells. All of the Ca^{2+} deficits noted in *Stim1*$^{-/-}$ cells were corrected by retroviral expression of STIM1. These observations provide direct evidence that mast cells exploit STIM1 for SOC influx, which serves an essential function in FcεRI-mediated Ca^{2+} responses.

The residual Ca^{2+} influx noted in *Stim1*$^{-/-}$ FLMCs may be explained by the expression of STIM2 (ref. 35) and/or by the coexistence of a SOC-independent Ca^{2+} influx pathway. Normal FcεRI-mediated PLC-γ activation and Ins(1,4,5)P_3 production in *Stim1*$^{-/-}$ mast cells support a model wherein STIM1 functions 'downstream' of PLC-γ and Ins(1,4,5)P_3 receptors in the pathway of FcεRI-mediated Ca^{2+} mobilization. However, it is noteworthy that the endoplasmic reticulum store depletion–related transient Ca^{2+} increase induced by antigen and thapsigargin was notably lower in *Stim1*$^{-/-}$ mast cells than in *Stim1*$^{+/+}$ mast cells. Because a chief function of SOC channels is believed to be maintenance of adequate endoplasmic reticulum Ca^{2+} stores, one likely explanation for these results is that dysfunction of

SOC activity in the absence of STIM1 resulted in insufficient replenishment of endoplasmic reticulum Ca^{2+} stores during the resting state in *Stim1*$^{-/-}$ FLMCs. Alternatively, it is possible that loss of STIM1 may affect the function of Ins(1,4,5)P_3 receptors or of the endoplasmic reticulum Ca^{2+} pump SERCA, thus leading to less release of Ca^{2+} from endoplasmic reticulum stores.

It has been shown that mast cells deficient in sphingosine kinase 2 (Sphk2) have a phenotype similar to that of *Stim1*$^{-/-}$ mast cells, with defective SOC influx, degranulation and cytokine production[36]. The diminished SOC influx in *Sphk2*$^{-/-}$ cells may be caused by defective conversion of sphingosine to sphingosine 1-phosphate, because *Sphk2*$^{-/-}$ mast cells have large amounts of sphingosine[36] that are known to inhibit SOC influx[37]. Thus, it is possible that sphingosine could prevent the functional association of STIM1 with SOC channels.

Mast cell degranulation was critically dependent on STIM1-mediated Ca^{2+} influx, and the initial release of Ca^{2+} from the endoplasmic reticulum stores was not sufficient to elicit degranulation. Mast cell degranulation involves granule translocation, granule docking and, ultimately, granule fusion with the plasma membrane[21]. The final fusion step requires Ca^{2+} (ref. 38). The SNARE family of membrane-fusion proteins is important for the fusion of these granules with the plasma membrane in mast cells[38,39]. Although SNARE proteins by themselves do not bind Ca^{2+}, the SNARE complex machinery contains Ca^{2+}-sensor proteins such as synaptotagmins and calmodulin, which promote membrane fusion through binding with Ca^{2+} (ref. 38). In addition, Ca^{2+}-dependent protein kinase C (PKC) may regulate membrane fusion through phosphorylation of the SNARE complex[38].

Although many reports have indicated the importance of Ca^{2+} flux in mast cell degranulation[20,21,38], Lyn-deficient mast cells show enhanced or normal degranulation despite defective Ca^{2+} mobilization[22–25]. Of particular note, however, Lyn-deficient mast cells showed delayed and prolonged but evident Ca^{2+} responses induced by antigen stimulation. In contrast, *Stim1*$^{-/-}$ mast cells showed a notable transient increase in Ca^{2+}, but no sustained Ca^{2+} increase. Thus, these observations suggest that a sustained Ca^{2+} increase is essential for mast cell degranulation. Alternatively, it is also possible that relatively high Ca^{2+} concentrations may be required in a local specialized region, such as docking sites between the plasma membrane and granules. Perhaps the Ca^{2+} concentrations in such specialized regions are sufficient in Lyn-deficient mast cells but insufficient in STIM1-deficient mast cells.

FcεRI ligation activates signaling cascades linking Lat with the adaptors Grb2 and SLP-76 that, by binding to the guanine nucleotide–exchange factors Sos and Vav, activate the GTPases Ras and Rac[40–42]. Subsequently, activated Ras and Rac initiate a signaling cascade that ultimately activates the MAP kinases Erk, p38 and Jnk[41,43–45]. Published reports have indicated that the PLC-γ–Ca^{2+}–PKC pathway also contributes to the activation of MAP kinases[43,45]. Supporting that possibility, our data also indicated that ionomycin-induced Ca^{2+} alone activated Erk, p38 and Jnk in *Stim1*$^{+/+}$ but not *Stim1*$^{-/-}$ FLMCs. After FcεRI stimulation, however, STIM1 deficiency had no effect on the activation of any of the MAP kinases, which indicated that FcεRI-induced MAP kinase activation occurs independently of Ca^{2+} influx.

The impaired production of IL-6, TNF and IL-13 by *Stim1*$^{-/-}$ mast cells is in agreement with the observed deficits in the activation of NF-κB[29,30] and NFAT[31,32], which regulate production of these cytokines in mast cells. In T lymphocytes and B lymphocytes, PKC-θ and PKC-β are important for NF-κB activation and function 'upstream' of the complex of adaptor proteins Bcl-10 and MALT1, respectively[46,47]. In mast cells, the PKC isoform(s) responsible for NF-κB activation has (have) not been defined. However, evidence from a study of PKC-β-deficient mast cells, in which IL-6 production was defective, suggests that this isoform could be a potential candidate[48,49]. Given that the activation of PKC-β is Ca^{2+} dependent, it is possible that NF-κB activation is regulated by STIM1-mediated Ca^{2+} influx via PKC-β. In addition to NF-κB, we also noted inhibition of the activation and nuclear localization of NFAT1 in *Stim1*$^{-/-}$ mast cells. In contrast to the residual FcεRI-mediated NF-κB activation in the absence of STIM1, NFAT activation seemed to be critically dependent on STIM1-mediated Ca^{2+} influx. These results confirm and extend the finding that NFAT requires a continuous increase in Ca^{2+} to remain localized in the nucleus[50,51].

Our *in vitro* observations were consistent with the defective IgE-mediated immediate-phase anaphylactic response in *Stim1*$^{-/-}$ mice. The functional importance of STIM1 in mast cells was shown by the impaired cutaneous allergic reaction measured by the PCA assay, as this reaction represents the activation of tissue mast cells in the skin. However, given the broad tissue distribution of STIM1 mRNA expression[52], a contribution of cells other than mast cells to the defective PCA responses remains possible. The SOC influx phenomenon was first described over 20 years ago[4,5], but the physiological importance has remained undefined. Here we have identified STIM1 as a critical positive regulator of SOC influx in mast cells and mast cell activity in hypersensitive reactions.

METHODS

Generation of *Stim1*$^{-/-}$ mice. Gene targeting and Cre-*lox*P–mediated recombination were used to generate mice with a null *Stim1* allele (*Stim1*$^{-/-}$). Additional details are in the **Supplementary Methods** online.

Antibodies. Antibodies specific for Syk (N-19; SC-1077), Lat (Q-20; SC-7548), Jnk (C-17; SC-474), p38 (C-20; SC-535), IκBα (C-21; SC-371), p65 (C-20; SC-372), β-actin (C-11; SC-1615) and NFAT1 (NFATc2; 4G6-65; SC-7269) were all from Santa Cruz Biotechnology. Antibody to phosphorylated Jnk (V793) and to phosphorylated p38 (V121) and anti-Erk1/2 (V114) were from Promega. Antibodies specific for PLC-γ1 (2822) and phosphorylated PLC-γ1 (2821), Syk (2711), IκBα (5A5), Lat and Erk (p42/44; 9101) were from Cell Signaling Technology; antibody to phosphorylated NFAT1 (ab5246) was from Abcam. Anti-STIM1 has been described[14]. Fluorescein isothiocyanate–conjugated anti-CD45.2 (104) and phycoerythrin-conjugated anti-FcεRI (MAR-1) were from BD Biosciences, and allophycocyanin-conjugated anti-c-Kit (2B8) was from eBioscience.

Mast cell culture. For the preparation of FLMCs, cell suspensions of fetal livers from E15.5 *Stim1*$^{+/+}$ and *Stim1*$^{-/-}$ embryos were cultured in RPMI 1640 medium supplemented with 10% (vol/vol) FCS, β-mercaptoethanol, antibiotics and recombinant mouse IL-3 (20 ng/ml; R&D Systems). The medium was changed every 3–4 d during culture. After 4–5 weeks of culture, cells were stained to confirm surface expression of FcεRI and c-Kit, then were used for experiments (over 98% mast cells).

Measurement of degranulation and cytokine production. Cells (1×10^6 cells/ml) were sensitized for 6 h at 37 °C with IgE anti-DNP (1 μg/ml; SPE-7; Sigma), then were stimulated for 30 min with polyvalent DNP-HSA (Sigma) in Tyrode's buffer (10 mM HEPES, pH 7.4, 130 mM NaCl, 5 mM KCl, 1.4 mM $CaCl_2$, 1 mM $MgCl_2$, 5.6 mM glucose and 0.1% (wt/vol) BSA). For the β-hexosaminidase reaction, 50 μl of supernatant or cell lysate was incubated with 100 μl of *p*-nitrophenyl-*N*-acetyl-D-glucosamide (1.3 mg/ml in 0.1 M citrate, pH 4.5), and color was developed for 60 min at 37 °C. The enzyme reaction was then stopped by the addition of 150 μl of 0.2 M glycine-NaOH, pH 10.2, and the absorbance at 405 nm was measured with a microplate reader (BioRad). Cells were lysed with Tyrode's buffer containing 1% (vol/vol) Triton X-100, and β-hexosaminidase activity was measured. The percent of β-hexosaminidase released was calculated with the following formula: release (%) = supernatant / (supernatant + cell lysate) × 100.

Degranulation was assessed by flow cytometry of surface expression of CD63. Additional details are in the **Supplementary Methods**. For measurement of cytokine release, IL-6, TNF and IL-13 in cell culture supernatants were detected by enzyme-linked immunosorbent assay as described[53].

Cell stimulation and immunoblot analysis. Cells (1×10^6 cells/ml) were sensitized for 6 h at 37 °C with IgE (1 μg/ml) and then were stimulated with DNP-HSA (50 ng/ml) in Tyrode's buffer. Alternatively, unsensitized cells were stimulated with 1 μM ionomycin. After stimulation, cells were lysed in lysis buffer containing 10 mM Tris-HCl, pH 7.4, 150 mM NaCl, 1% (vol/vol) Nonidet P-40, 0.1% (wt/vol) SDS, 0.5 mM EDTA and protease inhibitor (Roche) and phosphatase inhibitor (Nakarai) 'cocktails', and cleared cell lysates were boiled in 5× SDS sample buffer. Samples containing 5×10^5 to 1×10^6 cells were transferred to polyvinyldifluoride membranes by electrophoresis and were analyzed by immunoblot with the appropriate antibodies. Nuclear extracts were prepared with an Extraction Kit according to the manufacturer's protocol (Pierce) and were processed for immunoblot analysis.

Ca^{2+} measurement. Cytosolic Ca^{2+} concentrations were measured as described[14]. FLMCs were 'loaded' for 45 min at 37 °C with indo-1 acetoxylmethylester (Indo-1 AM) and Pluronic F-127 (Invitrogen) in RPMI 1640 medium containing 1% (vol/vol) FCS. For FcεRI stimulation, FLMCs were sensitized with IgE anti-DNP (2 μg/ml) simultaneously with the loading of Indo-1 AM. Changes in fluorescence intensity were monitored on an LSRII flow cytometer (BD Biosciences). Values were plotted as the ratio of fluorescence at FL5 (Ca^{2+}-bound Indo-1 AM) to that at FL4 (Ca^{2+}-free Indo-1 AM). Data were analyzed with FlowJo software (TreeStar).

Retrovirus production and infection. GFP-STIM1 cDNA[14] was cloned into the pMX-puro retroviral vector. The resulting vector and a control GFP-alone 'mock' vector were transfected into EcoPack2 cells (BD Biosciences) with FuGENE6 (Roche), and transfected cells were selected with puromycin (1.5 μg/ml). Supernatants were collected 24 h after the medium was changed and were immediately used for infection. For infection of FLMCs, cells were prestimulated for 16–18 h in the presence of recombinant mouse IL-3 (20 ng/ml) and recombinant mouse stem cell factor (20 ng/ml; R&D Systems). Cells then underwent 'spin infection' for 2 h at 32 °C and 800*g* after equal volumes of virus supernatant and the cationic lipid DOTAP (*N*-[1-(2, 3-dioleoyloxy)propyl]-*N*,*N*,*N*-trimethylammonium methyl-sulfate; 10 ng/ml; Roche) were added, and plates were incubated at 37 °C overnight. Culture medium was replaced the next day with fresh medium containing recombinant mouse IL-3.

PCA. PCA was achieved in mice as described[53]. Right ears were injected intradermally with 0.5 μg IgE anti-DNP in 20 μl saline and left ears were injected with 20 μl saline; 16–18 h later, mice were challenged by intravenous injection of 250 μg of polyvalent DNP-HSA in 250 μl of saline containing Evans blue dye (5 mg/ml; Sigma). Extravasation of Evans blue in the ear was monitored for 30 min, and ear biopsies were incubated at 63 °C overnight in 700 μl formamide. Quantitative analysis of formamide extracts was determined by measuring the absorbance of Evans blue at 620 nm.

Additional methods. Information on RT-PCR, histology, fetal liver transplantation, $Ins(1,4,5)P_3$ measurement, immunofluorescence and confocal microscopy is available in the **Supplementary Methods**.

Note: Supplementary information is available on the Nature Immunology website.

ACKNOWLEDGMENTS

We thank A. Ito for technical assistance; P.W. Kincade for critical review of the manuscript; and S. Yamasaki and H. Shinohara for discussions. The pMX-puro retroviral vector was from T. Kitamura (University of Tokyo). Supported the Ministry of Education, Culture, Sports, Science and Technology of Japan (Y.B. and T.K.).

AUTHOR CONTRIBUTIONS

Y.B. designed and coordinated the study, did experiments, analyzed data and wrote the paper; K.N., Y.F. and M.H. cooperated in experiments; T.K. wrote the paper; and T.H. contributed to manuscript writing.

Published online at http://www.nature.com/natureimmunology
Reprints and permissions information is available online at http://npg.nature.com/reprintsandpermissions

1. Wedemeyer, J., Tsai, M. & Galli, S.J. Roles of mast cells and basophils in innate and acquired immunity. *Curr. Opin. Immunol.* **12**, 624–631 (2000).
2. Bischoff, S.C. Role of mast cells in allergic and non-allergic immune responses: comparison of human and murine data. *Nat. Rev. Immunol.* **7**, 93–104 (2007).
3. Kraft, S. & Kinet, J.P. New developments in FcεRI regulation, function and inhibition. *Nat. Rev. Immunol.* **7**, 365–378 (2007).
4. Parekh, A.B. & Penner, R. Store depletion and calcium influx. *Physiol. Rev.* **77**, 901–930 (1997).
5. Parekh, A.B. & Putney, J.W., Jr. Store-operated calcium channels. *Physiol. Rev.* **85**, 757–810 (2005).
6. Clapham, D.E. TRP channels as cellular sensors. *Nature* **426**, 517–524 (2003).
7. Hoth, M. & Penner, R. Depletion of intracellular calcium stores activates a calcium current in mast cells. *Nature* **355**, 353–356 (1992).
8. Parekh, A.B., Fleig, A. & Penner, R. The store-operated calcium current I_{CRAC}: nonlinear activation by InsP3 and dissociation from calcium release. *Cell* **89**, 973–980 (1997).
9. Feske, S. *et al.* A mutation in Orai1 causes immune deficiency by abrogating CRAC channel function. *Nature* **441**, 179–185 (2006).
10. Vig, M. *et al.* CRACM1 is a plasma membrane protein essential for store-operated Ca^{2+} entry. *Science* **312**, 1220–1223 (2006).
11. Zhang, S.L. *et al.* Genome-wide RNAi screen of Ca^{2+} influx identifies genes that regulate Ca^{2+} release-activated Ca^{2+} channel activity. *Proc. Natl. Acad. Sci. USA* **103**, 9357–9362 (2006).
12. Roos, J. *et al.* STIM1, an essential and conserved component of store-operated Ca^{2+} channel function. *J. Cell Biol.* **169**, 435–445 (2005).
13. Liou, J. *et al.* STIM is a Ca^{2+} sensor essential for Ca^{2+}-store-depletion-triggered Ca^{2+} influx. *Curr. Biol.* **15**, 1235–1241 (2005).
14. Baba, Y. *et al.* Coupling of STIM1 to store-operated Ca^{2+} entry through its constitutive and inducible movement in the endoplasmic reticulum. *Proc. Natl. Acad. Sci. USA* **103**, 16704–16709 (2006).
15. Luik, R.M. & Lewis, R.S. New insights into the molecular mechanisms of store-operated Ca^{2+} signaling in T cells. *Trends Mol. Med.* **13**, 103–107 (2007).
16. Mercer, J.C. *et al.* Large store-operated calcium selective currents due to co-expression of Orai1 or Orai2 with the intracellular calcium sensor, Stim1. *J. Biol. Chem.* **281**, 24979–24990 (2006).
17. Xu, P. *et al.* Aggregation of STIM1 underneath the plasma membrane induces clustering of Orai1. *Biochem. Biophys. Res. Commun.* **350**, 969–976 (2006).
18. Wu, M.M., Buchanan, J., Luik, R.M. & Lewis, R.S. Ca^{2+} store depletion causes STIM1 to accumulate in ER regions closely associated with the plasma membrane. *J. Cell Biol.* **174**, 803–813 (2006).
19. Stathopulos, P.B., Li, G.Y., Plevin, M.J., Ames, J.B. & Ikura, M. Stored Ca^{2+} depletion-induced oligomerization of stromal interaction molecule 1 (STIM1) via the EF-SAM region: an initiation mechanism for capacitive Ca^{2+} entry. *J. Biol. Chem.* **281**, 35855–35862 (2006).
20. Ozawa, K. *et al.* Ca^{2+}-dependent and Ca^{2+}-independent isozymes of protein kinase C mediate exocytosis in antigen-stimulated rat basophilic RBL-2H3 cells. Reconstitution of secretory responses with Ca^{2+} and purified isozymes in washed permeabilized cells. *J. Biol. Chem.* **268**, 1749–1756 (1993).
21. Nishida, K. *et al.* FcεRI-mediated mast cell degranulation requires calcium-independent microtubule-dependent translocation of granules to the plasma membrane. *J. Cell Biol.* **170**, 115–126 (2005).
22. Odom, S. *et al.* Negative regulation of immunoglobulin E-dependent allergic responses by Lyn kinase. *J. Exp. Med.* **199**, 1491–1502 (2004).
23. Parravicini, V. *et al.* Fyn kinase initiates complementary signals required for IgE-dependent mast cell degranulation. *Nat. Immunol.* **3**, 741–748 (2002).
24. Nishizumi, H. & Yamamoto, T. Impaired tyrosine phosphorylation and Ca^{2+} mobilization, but not degranulation, in lyn-deficient bone marrow-derived mast cells. *J. Immunol.* **158**, 2350–2355 (1997).
25. Hernandez-Hansen, V. *et al.* Dysregulated FcεRI signaling and altered Fyn and SHIP activities in Lyn-deficient mast cells. *J. Immunol.* **173**, 100–112 (2004).
26. Putney, J.W., Jr. Store-operated calcium channels: how do we measure them, and why do we care? *Sci. STKE* **2004**, pe37 (2004).
27. Hofer, A.M., Fasolato, C. & Pozzan, T. Capacitative Ca^{2+} entry is closely linked to the filling state of internal Ca^{2+} stores: a study using simultaneous measurements of I_{CRAC} and intraluminal. *J. Cell Biol.* **140**, 325–334 (1998).
28. Siraganian, R.P. Mast cell signal transduction from the high-affinity IgE receptor. *Curr. Opin. Immunol.* **15**, 639–646 (2003).
29. Klemm, S. *et al.* The Bcl10-Malt1 complex segregates FcεRI-mediated nuclear factor κB activation and cytokine production from mast cell degranulation. *J. Exp. Med.* **203**, 337–347 (2006).
30. Chen, Y. *et al.* B cell lymphoma 10 is essential for FcεR-mediated degranulation and IL-6 production in mast cells. *J. Immunol.* **178**, 49–57 (2007).
31. Monticelli, S., Solymar, D.C. & Rao, A. Role of NFAT proteins in IL13 gene transcription in mast cells. *J. Biol. Chem.* **279**, 36210–36218 (2004).
32. Klein, M. *et al.* Specific and redundant roles for NFAT transcription factors in the expression of mast cell-derived cytokines. *J. Immunol.* **177**, 6667–6674 (2006).

33. Dolmetsch, R.E., Lewis, R.S., Goodnow, C.C. & Healy, J.I. Differential activation of transcription factors induced by Ca^{2+} response amplitude and duration. *Nature* **386**, 855–858 (1997).
34. Healy, J.I. *et al.* Different nuclear signals are activated by the B cell receptor during positive versus negative signaling. *Immunity* **6**, 419–428 (1997).
35. Dziadek, M.A. & Johnstone, L.S. Biochemical properties and cellular localisation of STIM proteins. *Cell Calcium* **42**, 123–132 (2007).
36. Olivera, A. *et al.* The sphingosine kinase-sphingosine-1-phosphate axis is a determinant of mast cell function and anaphylaxis. *Immunity* **26**, 287–297 (2007).
37. Mathes, C., Fleig, A. & Penner, R. Calcium release-activated calcium current (I_{CRAC}) is a direct target for sphingosine. *J. Biol. Chem.* **273**, 25020–25030 (1998).
38. Blank, U. & Rivera, J. The ins and outs of IgE-dependent mast-cell exocytosis. *Trends Immunol.* **25**, 266–273 (2004).
39. Bonifacino, J.S. & Glick, B.S. The mechanisms of vesicle budding and fusion. *Cell* **116**, 153–166 (2004).
40. Manetz, T.S. *et al.* Vav1 regulates phospholipase cgamma activation and calcium responses in mast cells. *Mol. Cell. Biol.* **21**, 3763–3774 (2001).
41. Saitoh, S. *et al.* The four distal tyrosines are required for LAT-dependent signaling in FcεRI-mediated mast cell activation. *J. Exp. Med.* **198**, 831–843 (2003).
42. Pivniouk, V.I. *et al.* SLP-76 deficiency impairs signaling via the high-affinity IgE receptor in mast cells. *J. Clin. Invest.* **103**, 1737–1743 (1999).
43. Hashimoto, A. *et al.* Involvement of guanosine triphosphatases and phospholipase C-γ2 in extracellular signal-regulated kinase, c-Jun NH_2-terminal kinase, and p38 mitogen-activated protein kinase activation by the B cell antigen receptor. *J. Exp. Med.* **188**, 1287–1295 (1998).
44. Hirasawa, N., Santini, F. & Beaven, M.A. Activation of the mitogen-activated protein kinase/cytosolic phospholipase A2 pathway in a rat mast cell line. Indications of different pathways for release of arachidonic acid and secretory granules. *J. Immunol.* **154**, 5391–5402 (1995).
45. Jiang, A., Craxton, A., Kurosaki, T. & Clark, E.A. Different protein tyrosine kinases are required for B cell antigen receptor-mediated activation of extracellular signal-regulated kinase, c-Jun NH_2-terminal kinase 1, and p38 mitogen-activated protein kinase. *J. Exp. Med.* **188**, 1297–1306 (1998).
46. Schulze-Luehrmann, J. & Ghosh, S. Antigen-receptor signaling to nuclear factor κB. *Immunity* **25**, 701–715 (2006).
47. Shinohara, H. *et al.* PKCβ regulates BCR-mediated IKK activation by facilitating the interaction between TAK1 and CARMA1. *J. Exp. Med.* **202**, 1423–1431 (2005).
48. Nechushtan, H., Leitges, M., Cohen, C., Kay, G. & Razin, E. Inhibition of degranulation and interleukin-6 production in mast cells derived from mice deficient in protein kinase Cβ. *Blood* **95**, 1752–1757 (2000).
49. Rivera, J. Adaptors discriminate mast-cell cytokine production from eicosanoid production and degranulation. *Trends Immunol.* **27**, 251–253 (2006).
50. Timmerman, L.A., Clipstone, N.A., Ho, S.N., Northrop, J.P. & Crabtree, G.R. Rapid shuttling of NF-AT in discrimination of Ca^{2+} signals and immunosuppression. *Nature* **383**, 837–840 (1996).
51. Shibasaki, F., Price, E.R., Milan, D. & McKeon, F. Role of kinases and the phosphatase calcineurin in the nuclear shuttling of transcription factor NF-AT4. *Nature* **382**, 370–373 (1996).
52. Oritani, K. & Kincade, P.W. Identification of stromal cell products that interact with pre-B cells. *J. Cell Biol.* **134**, 771–782 (1996).
53. Kabu, K. *et al.* Zinc is required for FcεRI-mediated mast cell activation. *J. Immunol.* **177**, 1296–1305 (2006).